

Spontaneous Spin Textures in Dipolar Spinor Condensates: A Dirac String Gas Approach

Biao Lian

Department of Physics, McCullough Building, Stanford University, Stanford, California 94305-4045, USA

(Dated: October 21, 2018)

We study the spontaneous spin textures induced by magnetic dipole-dipole interaction in ferromagnetic spinor condensates under various trap geometries. At the mean-field level, we show the system is dual to a Dirac string gas with a negative string tension in which the ground state spin texture can be easily determined. We find that three-dimensional condensates prefer a meron-like vortex texture, quasi one-dimensional condensates prefer the axially polarized flare texture, while condensates in quasi two dimensions exhibit either a meron texture or an in-plane polarized texture.

I. INTRODUCTION

The magnetic dipole-dipole interaction (DDI) is known to play a significant role in determining the long range behaviors of ultracold gases of spinful atoms, especially those with a large spin [1–3]. In the ferromagnetic spinor condensates of spinful bosons with nonzero spin expectation values $\langle \mathbf{F} \rangle$, the DDI usually leads to rich spin textures that strongly depend on the trap geometry and the initial state preparation [4–7]. Meanwhile, the existence of spontaneous spin textures in dipolar spinor condensates has been verified by numerical simulations based on the mean-field Gross-Pitaevskii equation [8–12]. However, due to the complicated form of DDI, there still lacks an explicit and efficient theoretical way to understand the spin textures.

In this letter, we develop an semi-analytical approach to the problem by introducing a duality at the mean-field level from a strong dipolar spinor condensate to a weakly interacting Dirac string gas with a negative string tension. We find that the ground state is reached by forming as many closed strings with small enough curvatures as possible. Based on this principle, we are able to determine the spin textures in various trap geometries used in cold atom experiments. We show the ground state spin texture of a large three-dimensional (3D) spherical condensate is a meron-like vortex texture. Further, we show the axially polarized flare texture [10] is favored in quasi one-dimensional (1D) condensates, while in quasi two-dimensional (2D) pancake traps there is a phase transition between an in-plane polarized texture and a meron texture driven by the pancake radius. In particular, multiple merons can be seen to arise in quasi 2D traps when the aspect ratio is comparatively large, in agreement with the numerical results in Ref. [9]. The Dirac string gas picture thus offers a greatly simplified way to understand the spin textures in dipolar condensates.

II. THEORETICAL FORMULATION

We begin with the description of the ferromagnetic spinor condensates at low energies. In general, a spinor condensate of integral spin F atoms is characterized by

a spinor order parameter of $2F + 1$ components $\Psi_m(\mathbf{r})$ ($m = -F, -F + 1, \dots, F$), which represents the coherent amplitude of annihilating a boson in the spin state $|F, m\rangle$ at position \mathbf{r} [13–16]. At the mean field level, the number of atoms per unit volume in the condensate is $n(\mathbf{r}) = \sum_m \Psi_m^*(\mathbf{r})\Psi_m(\mathbf{r}) = \Psi^\dagger(\mathbf{r})\Psi(\mathbf{r})$, while the expectation of the local spin is $\langle \mathbf{F}(\mathbf{r}) \rangle = \varphi^\dagger(\mathbf{r})\mathbf{F}\varphi(\mathbf{r})$, where $\varphi(\mathbf{r}) = \Psi(\mathbf{r})/\sqrt{n(\mathbf{r})}$ is the normalized spinor order parameter, and \mathbf{F} is the spin matrix of the spin F representation. In a square well trap potential or in the central region of a harmonic trap within a size $R \ll n(\mathbf{r})/|\nabla n(\mathbf{r})|$, we can approximate the particle number density $n(\mathbf{r}) = n_0$ as a constant. Up to a $U(1) \times SU(2)$ transformation, the normalized spinor order parameter $\varphi(\mathbf{r})$ is determined by the local interactions, which are characterized by $F + 1$ scattering lengths a_{2J} between two atoms with total spin $2J$ ($0 \leq J \leq F$) [16]. A spinor condensate is said to be ferromagnetic if $\varphi(\mathbf{r}) = (0, \dots, 0, 1, 0, \dots, 0, 0)$ in a certain basis, where the only nonzero component is $m = F_0 > 0$.

At low energies, the long wave length fluctuation of the order parameter gives rise to multiple gapless Goldstone modes. In a ferromagnetic spinor condensate, there is exactly one quadratic dispersion mode corresponding to the fluctuation of the local spin [13–16]. In the presence of the magnetic dipole-dipole interaction, the effective low energy spin Hamiltonian of a ferromagnetic spinor condensate can be written as $H = H_0 + H_D$, where

$$\begin{aligned} H_0 &= \frac{\alpha}{M} \int d^3\mathbf{r} (\nabla \mathcal{F}(\mathbf{r}))^2, \\ H_D &= \frac{\lambda}{2} \int d^3\mathbf{r}_1 d^3\mathbf{r}_2 \frac{\mathcal{F}_1 \cdot \mathcal{F}_2 - 3(\mathcal{F}_1 \cdot \hat{\mathbf{r}}_{12})(\mathcal{F}_2 \cdot \hat{\mathbf{r}}_{12})}{4\pi r_{12}^3} \end{aligned} \quad (1)$$

are the kinetic energy of the quadratic Goldstone mode and the DDI energy, respectively (see Appendix A). We have used here the normalized local spin field $\mathcal{F}(\mathbf{r}) = \langle \mathbf{F}(\mathbf{r}) \rangle / F_0$ that satisfies $|\mathcal{F}(\mathbf{r})| = 1$ for later convenience. M denotes the particle mass, α is defined by $\alpha = n_0 \hbar^2 [F(F + 1) - F_0^2] / 4$, and the interaction parameter λ is given by $\lambda = \mu_0 (g_F \mu_B)^2 n_0^2 F_0^2$, where g_F is the Landé factor and μ_B is the Bohr magneton. In writing the H_D term, we have used the abbreviations $\mathcal{F}_i = \mathcal{F}(\mathbf{r}_i)$ and $\mathbf{r}_{12} = r_{12} \hat{\mathbf{r}}_{12} = \mathbf{r}_1 - \mathbf{r}_2$, where $\hat{\mathbf{r}}_{12}$ is the corresponding

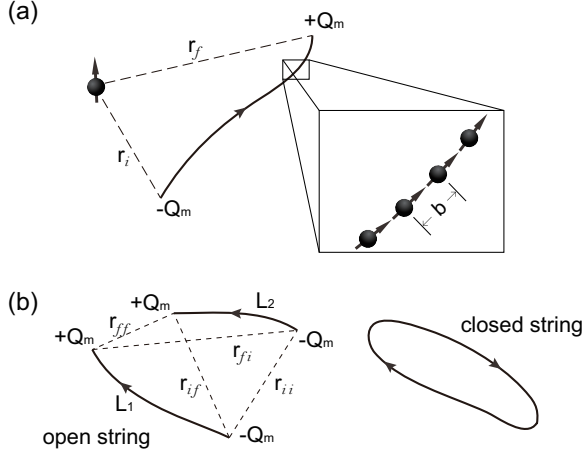


FIG. 1. (a) A single column chain of head-to-tail spins is equivalent to a Dirac string with two monopoles $\pm Q_m$ at the ends. (b) Under the dipolar interaction of spins, two open strings only have an interaction between the monopoles, while closed strings are free.

unit vector.

It is difficult to infer the low energy spin texture configurations directly from the perspective of local spins, since the spin-spin interaction in H_D is highly anisotropic. However, it is possible to understand H_D more naturally in terms of Dirac strings. Consider a chain of atoms that are arranged uniformly along a curve as is shown in Fig. 1(a), with their spins aligned head-to-tail and parallel to the tangent of the curve. Since each atom carries a magnetic dipole moment $\mathbf{m}_F = g_F \mu_B \langle \mathbf{F} \rangle$, the curve can be exactly viewed as a Dirac string, with a positive magnetic monopole at one end and a negative one at the other. If we parameterize the curve as $\mathbf{r}(l)$ with an affine parameter l , and require $|\mathbf{dr}/dl| = 1$, the local spin field on the curve is then $\mathcal{F} = \mathbf{dr}/dl$. We can easily calculate the dipolar interaction between such a Dirac string and a spin magnetic moment \mathbf{m}_F not belonging to the string:

$$E_{\mathbf{m}_F} = \mu_0 Q_m \int dl \frac{r^2 \mathbf{m}_F \cdot \frac{\mathbf{dr}}{dl} - 3(\mathbf{m}_F \cdot \mathbf{r})(\mathbf{r} \cdot \frac{\mathbf{dr}}{dl})}{4\pi r^5} \quad (2)$$

$$= \mu_0 Q_m \left(\frac{\mathbf{r}_f}{4\pi r_f^3} - \frac{\mathbf{r}_i}{4\pi r_i^3} \right) \cdot \mathbf{m}_F = -\mathbf{m}_F \cdot \mathbf{B}_{str}$$

where we have defined $Q_m = g_F \mu_B F_0 / b$ with the spacing between atoms on the string $b \sim n_0^{-1/3}$, while \mathbf{r}_i and \mathbf{r}_f are the positions of the ends of the string relative to \mathbf{m}_F . This means that effectively the magnetic moment \mathbf{m}_F only feels the magnetic field of the monopoles at the ends of the string, which carry monopole charges $\pm Q_m$ respectively. Remarkably, a closed Dirac string has no interaction energy with the other spins at all.

Further, it is straightforward to prove that the interaction energy between two Dirac strings is solely given by the interaction between the four monopoles at the ends of the strings. Consider two strings L_1 and L_2 as shown

in Fig. 1(b), whose ends are located at \mathbf{r}_i , \mathbf{r}_f and \mathbf{r}'_i , \mathbf{r}'_f respectively. We shall parameterize string L_1 as $\mathbf{r}(l)$, and use the abbreviations $\mathbf{r}_i(l) = \mathbf{r}'_i - \mathbf{r}(l)$, $\mathbf{r}_f(l) = \mathbf{r}'_f - \mathbf{r}(l)$ to denote the displacement vectors from $\mathbf{r}(l)$ to the ends of string L_2 . The magnetic moment of an infinitesimal segment dl on string L_1 is then $\mathbf{m}_F = g_F \mu_B F_0 \mathbf{dr}(l)/b = Q_m \mathbf{dr}(l) = -Q_m \mathbf{dr}_i(l) = -Q_m \mathbf{dr}_f(l)$. According to the result of Eq. (2), the total DDI energy between the two strings is simply

$$E_Q(L_1, L_2) = \mu_0 Q_m^2 \int \mathbf{dr}(l) \left[\frac{\mathbf{r}_f(l)}{4\pi r_f(l)^3} - \frac{\mathbf{r}_i(l)}{4\pi r_i(l)^3} \right]$$

$$= \mu_0 Q_m^2 \left[-\int_{\mathbf{r}_{if}}^{\mathbf{r}_{ff}} \frac{\mathbf{r}_f(l) \mathbf{dr}_f(l)}{4\pi r_f(l)^3} + \int_{\mathbf{r}_{ii}}^{\mathbf{r}_{fi}} \frac{\mathbf{r}_i(l) \mathbf{dr}_i(l)}{4\pi r_i(l)^3} \right] \quad (3)$$

$$= \frac{\mu_0 Q_m^2}{4\pi} \left(\frac{1}{r_{ff}} - \frac{1}{r_{if}} - \frac{1}{r_{fi}} + \frac{1}{r_{ii}} \right),$$

where r_{ff} , r_{if} , r_{fi} and r_{ii} are the distances between monopoles at the ends of the two strings as shown in Fig. 1(b). The interaction energy between two monopoles is thus simply given by the Coulomb law. Accordingly, two parallel(anti-parallel) Dirac strings will repulse(attract) each other. Still, a closed string does not interact with any other strings. Therefore, the Dirac strings are almost free under DDI except for the monopole interactions between their ends.

In the continuum limit, we can view the flow lines of the local spin field $\mathcal{F}(\mathbf{r})$ of the condensate as Dirac strings, each of which consists of a single column of atoms. We denote the cross sectional area of a string as $d\sigma$, which is around $n_0^{-2/3}$. The spacing between atoms on a string is then $b = (n_0 d\sigma)^{-1}$, and the monopole charge can be expressed as $Q_m = g_F \mu_B n_0 F_0 d\sigma$, which is proportional to the cross sectional area $d\sigma$.

So far we have seen the bulk of a Dirac string has no interaction with other strings at all under DDI. However, as we shall shown in the below, a Dirac string has a negative self-interaction bulk energy coming from the DDI. To understand the origin of the self-interaction energy, consider a straight Dirac string of length L . Since all the spins are aligned head-to-tail, there is an attractive DDI energy $-2(\lambda/n_0^2)(1/4\pi r^3)$ between any two of them, where r is the distance between them. This gives rise to the self-interaction energy of the string. In the limit $b \ll L$, the attraction energy felt by a spin on the string is approximately

$$E_{F_0} \approx -\frac{\lambda}{n_0^2} \sum_{N=1}^{\infty} \frac{1}{\pi} \left(\frac{1}{Nb} \right)^3 \propto -\frac{\lambda}{n_0},$$

where we have used the fact $1/b^3 \propto n_0$. Thus, the self-attraction energy E_{F_0} of each spin is a constant not sensitive to the string length L .

The above estimation, however, cannot give the coefficient in front of $-\lambda/n_0$ in the expression of E_{F_0} , since we do not know the exact relation between $1/b^3$ and n_0 in

the continuum limit. Instead, we can find out the coefficient by directly computing the DDI energy of a simple concrete example of spin texture. Consider a 3D spherical condensate with all spins polarized along z direction as shown in Fig. 2(a). The total DDI energy E_d felt by the spin at the center can be directly calculated in spherical coordinates from its definition:

$$E_d = \frac{\lambda}{n_0} \int_0^R 2\pi r^2 dr \int_0^\pi d\theta \sin\theta \frac{1 - 3\cos^2\theta}{4\pi r^3} = 0, \quad (4)$$

where R is the trap radius, and θ is the polar angle. On the other hand, in the picture of Dirac strings, the DDI energy E_d felt by the spin consists of the attraction energy E_{F_0} from its own string and the interaction with monopoles at the ends of all the strings derived in Eq. (2). In cylindrical coordinates (ρ, ϕ, z) , the cross sectional area of a string is $d\sigma = \rho d\rho d\phi$, and this energy is calculated as

$$E_d = E_{F_0} + \frac{2\lambda}{n_0} \int_0^R 2\pi \rho d\rho \frac{\sqrt{R^2 - \rho^2}}{4\pi R^3} = E_{F_0} + \frac{\lambda}{3n_0}. \quad (5)$$

By equalizing Eq. (4) and Eq. (5), we see the attraction energy

$$E_{F_0} = -\frac{\lambda}{3n_0}.$$

The total self-interaction energy of a Dirac string of length L and of cross sectional area $d\sigma$ is then

$$E_{str}^{(d)}(L) = \frac{E_{F_0}}{2} \times n_0 L d\sigma = -\frac{1}{6} \lambda L d\sigma. \quad (6)$$

This indicates that a Dirac string has a negative string tension $T_{str} = -\lambda d\sigma/6$, and therefore the whole space will prefer to be filled with Dirac strings. The action for a single Dirac string can be written as $\mathcal{S}_{str} = (T_{str}/\hbar) \int dt dl = T_{str} \Sigma/\hbar$, where Σ is the worldsheet area of the string. The Dirac string therefore corresponds to a classical bosonic string theory with a $U(1)$ gauge group [17].

Now we turn to the kinetic energy H_0 in Eq. (1), and interpret it in the language of Dirac strings. By writing the gradient operator into $\nabla = \nabla_{\parallel} + \nabla_{\perp}$, where \parallel and \perp stands for parallel and perpendicular to the string respectively, we can divide H_0 into the following two parts: the first parallel part contributes an additional term to the string self energy. This is seen by noticing that $\nabla_{\parallel} \mathcal{F} = d\mathcal{F}/dl = d^2\mathbf{r}/dl^2$, so the string self energy now reads

$$E_{str}(L) = d\sigma \int_0^L dl \left[-\frac{1}{6} \lambda + \frac{\alpha}{M} \left(\frac{d^2\mathbf{r}}{dl^2} \right)^2 \right]. \quad (7)$$

Note that $|d^2\mathbf{r}/dl^2|$ is the curvature of the string. The second perpendicular part induces a nonnegative contact interaction between two Dirac strings L_1 and L_2 (see

Appendix B):

$$E_I(L_1, L_2) = d\sigma_1 d\sigma_2 \frac{\alpha}{M} \int_0^{L_1} dl_1 \int_0^{L_2} dl_2 \times \left(1 - \frac{d\mathbf{r}_1}{dl_1} \cdot \frac{d\mathbf{r}_2}{dl_2} \right) \nabla_{\perp}^2 \delta(\mathbf{r}_1 - \mathbf{r}_2), \quad (8)$$

where ∇_{\perp}^2 is defined as $\nabla_{\perp}^2 = \nabla^2 - \partial_{l_1}^2$, and $\mathbf{r}_1 = \mathbf{r}_1(l_1)$, $\mathbf{r}_2 = \mathbf{r}_2(l_2)$. Though looks complicated, this contact interaction simply implies that two nearby Dirac strings prefer to be coplanar, namely, $|d\mathbf{r}_1/dl_1 - d\mathbf{r}_2/dl_2|/|\mathbf{r}_1 - \mathbf{r}_2| \rightarrow 0$ as $|\mathbf{r}_1 - \mathbf{r}_2| \rightarrow 0$.

Therefore, we have seen the ferromagnetic dipolar condensate at the mean-field level is dual to a Dirac string gas with a string self energy E_{str} , a monopole interaction energy E_Q and a contact interaction energy E_I , given in Eq. (7), Eq. (3) and Eq. (8), respectively. With E_{str} mainly coming from the DDI H_D and E_I coming from H_0 , such a duality between individual spins and Dirac strings interchanges the roles of the kinetic energy and the interaction energy in some sense, and is thus a strong-weak duality.

III. APPLICATION TO SPHERICAL TRAP GEOMETRIES

The ground state spin texture can be more easily derived in the Dirac string gas picture. First, since an open string can always lower its monopole interaction energy by attaching its two ends together and forming a closed string, a strong dipolar condensate will prefer as many closed strings as possible. Further, to reduce the kinetic energy H_0 , the close strings will tend to have a smaller average curvature and be locally coplanar to each other. These facts constitute the guiding rules for identifying the spin textures in a condensate under various trap geometries.

We first consider a dipolar condensate in a 3D spherical square well trap potential of radius R . Based on the guiding rules above, the most natural spin texture one can expect is a meron-like vortex texture as shown in Fig. 2(b). Since circular closed strings possess the smallest average curvature, the region $\rho > R_0$ (in cylindrical coordinates) prefers to be filled with circular strings parallel to each other, where R_0 is a characteristic length scale to be determined. All the circular strings are symmetric about the z axis, so that locally they are always coplanar. At $\rho < R_0$, the circular strings will have too large curvatures, and thus will gradually give way to spiral strings proceeding along the z direction to lower the kinetic energy H_0 . Finally, the string becomes vertical and straight at the central axis $\rho = 0$. Consequently, there will be monopoles distributed on the $\rho < R_0$ regions of the sphere's surface, with a monopole area density $n_A \approx \pm Q_m/d\sigma = \pm g_F \mu_B n_0 F_0$. The total energy of

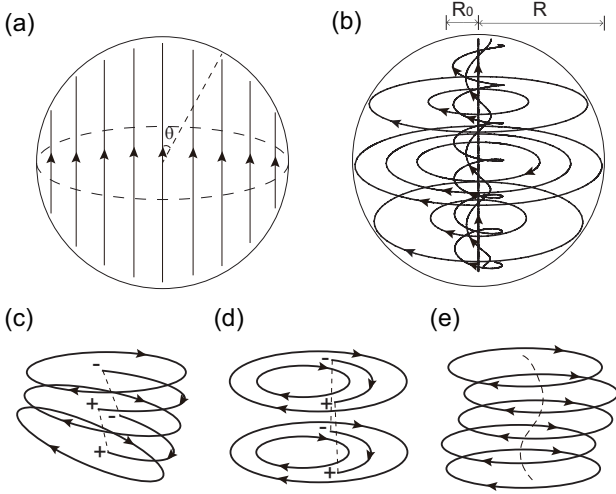


FIG. 2. (a) In the absence of dipolar interaction, all the spins will be polarized along the same direction. (b) The meron-like vortex spin texture of spherical dipolar condensates. (c), (d) and (e) shows several perturbation patterns that may arise in the spin texture, all of which increase the total energy.

the dipolar condensate can be estimated as

$$E_{3D} \approx -\frac{\lambda}{6}V + \int_{\rho \geq R_0}^R d^3\mathbf{r} \frac{\alpha}{M} \frac{1}{\rho^2} + \frac{2\mu_0(\pi R_0^2 n_A)^2}{4\pi R_0} \quad (9)$$

$$\approx -\frac{\lambda}{6}V + \frac{4\pi\alpha}{M}R \log \frac{R}{R_0} + \frac{\pi}{2}\lambda R_0^3,$$

where $V = 4\pi R^3/3$ is the volume of the condensate, and R_0/R is assumed small. The second term is the kinetic energy H_0 mainly coming from the curvatures of the strings, while the third term is the monopole interaction energy estimated by taking R_0 as the average distance between monopoles [18]. By minimizing the total energy with respect to R_0 , we get the characteristic length

$$R_0 = (8\alpha/3\lambda M)^{1/3} R^{1/3}.$$

The condition for the meron-like spin texture to arise is then roughly $R > R_0$, or $R > (8\alpha/3\lambda M)^{1/2}$. Therefore, the spin textures are more likely to arise for massive and large spin atoms.

It is easy to see the meron-like spin texture is energetically stable. When perturbed, the circular strings may be tilted, misaligned, or distorted. In any case, the total energy is raised higher. In the examples shown in Fig. 2(c) and Fig. 2(d), parallel open strings have to arise to keep the strings dense, which then cost an extra monopole interaction energy. In another case shown in Fig. 2(e), no monopole occurs, but the strings are no longer locally coplanar to each other, which also increases the kinetic energy H_0 . These perturbation patterns may have interesting dynamics, which is open to studies in the future.

To verify the precision of our estimation above, we perform a numerical calculation based on the following

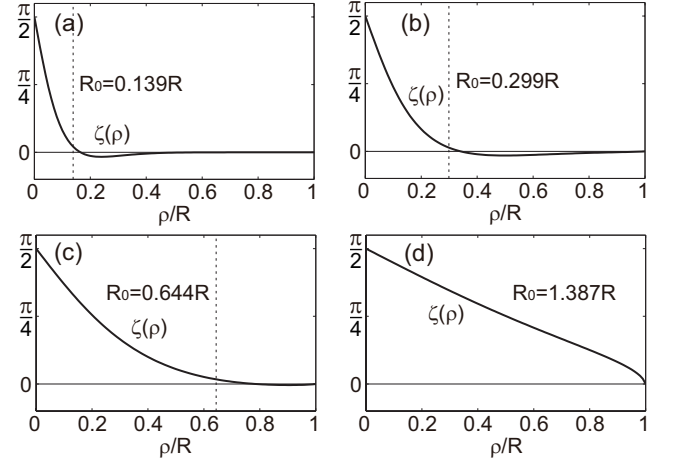


FIG. 3. The ground state angle function $\zeta(\rho)$ calculated for different values of $R_0 = (8\alpha/3\lambda M)^{1/3} R^{1/3}$. The dashed lines denote the positions of R_0 . When $R_0 < R$, R_0 is a rather precise boundary separating the $\zeta(\rho) \neq 0$ region and the $\zeta(\rho) \approx 0$ region.

spin texture ansatz, expressed in cylindrical coordinates (ρ, ϕ, z) as:

$$\mathcal{F}(\mathbf{r}) = \mathbf{e}_\phi \cos \zeta(\rho) + \mathbf{e}_z \sin \zeta(\rho), \quad (10)$$

where $\zeta(\rho)$ is a function of ρ only. This ansatz simply describes the spin texture shown in Fig. 2(b). $\zeta(\rho)$ has the physical meaning of the proceeding angle of a spiral string at radius ρ , and the string becomes circular when $\zeta(\rho) = 0$. Fig. 3 shows $\zeta(\rho)$ calculated numerically for various values of R_0 , and the details of the calculations can be found in Appendix C. As is seen, our estimation of R_0 gives a rather precise boundary between the region of spiral strings ($\zeta(\rho) \neq 0$) and the region of circular strings ($\zeta(\rho) \approx 0$), even for R_0/R that is no longer very small.

IV. APPLICATIONS TO CIGAR AND PANCAKE TRAP GEOMETRIES

This analysis can be readily applied to the dipolar condensates in other trap geometries. A practical and important geometry is the axially symmetric square well trap where the boundary is given by $x^2 + y^2 + (z/A)^2 = R^2$. By setting $A \gg 1$, we get a quasi-1D cigar trap of length $L_c = 2AR$. In the extremely quasi-1D case, closed strings are no longer energetically favorable, since their curvatures are always too large. Instead, vertical strings along z direction are preferred, so that the amount of monopoles on the surface is minimal and the monopole energy is the smallest. In a realistic trap, the particle number density n_0 is not constant and usually lower near the surface. To validate our theoretical formulation in Sec. II, we need to keep $b = (n_0 d\sigma)^{-1}$ constant for a string, so the effective cross sectional area density of strings $n_s \sim 1/d\sigma \propto n_0$ is also lower near the surface. In

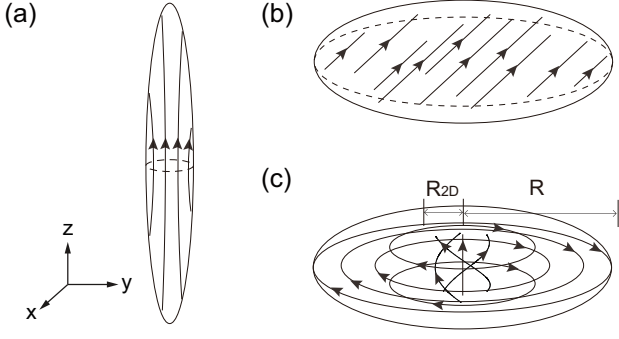


FIG. 4. (a) The flare texture in a quasi-1D cigar trap. (b) The in-plane polarized texture in a quasi-2D pancake trap. (c) The meron texture in the pancake trap.

the cigar trap case, the vertical strings are then forced to be bent outward to have a lower density near the surface, forming a flare texture as shown in Fig. 4(a). By an energy estimation similar to what we did for spherical traps, one can show that circular closed strings begin to occur when $A \sim (\lambda M/\alpha)^{1/3} L_c^{2/3}$ or smaller, leading to a crossover from the flare texture to the 3D meron-like vortex texture.

In the opposite limit $A \ll 1$, the trap is a quasi-2D pancake of radius R . Correspondingly, there are two candidate ground state spin textures. The first spin texture is shown in Fig. 4(b), where all strings are in-plane and polarized along the same direction to minimize the amount of surface monopoles. The total energy of this texture consists of the string self-energy and the surface monopole interaction energy, or explicitly

$$E_{2D}^{(I)} \approx -\frac{\lambda}{6}V + w\lambda R^3 A^2 \log \frac{1}{A}, \quad (11)$$

where V is the volume of the condensate, and $w > 0$ is a numerical factor. The second spin texture is the 2D meron texture shown in Fig. 4(c). Similar to the 3D case, there is a characteristic radius R_{2D} . The region outside R_{2D} is filled with in-plane circular strings, while inside R_{2D} strings become spiral and finally vertical at the center. In the case the half height of the pancake $z_h = AR \ll R_{2D}$, the total energy of the configuration can be estimated as [19]

$$E_{2D}^{(II)} \approx -\frac{\lambda}{6}V + \frac{4\pi\alpha}{M}z_h \log \frac{R}{R_{2D}} + \frac{\pi\lambda}{2}z_h R_{2D}^2. \quad (12)$$

Minimizing the energy we get $R_{2D} = (4\alpha/\lambda M)^{1/2}$, which is independent of z_h or R . At a fixed half height z_h , one can show that the in-plane polarized texture is favored when $R < R_c$, where R_c is a critical radius determined by solving $E_{2D}^{(I)} = E_{2D}^{(II)}$, while the meron texture arises when $R > R_c$. We note the two textures are separated by a phase transition at $R = R_c$ instead of a crossover.

When the pancake trap is not axially symmetric, multiple merons may occur. As an example, in a rectangular trap with aspect ratio $q = 2$, the single-meron texture

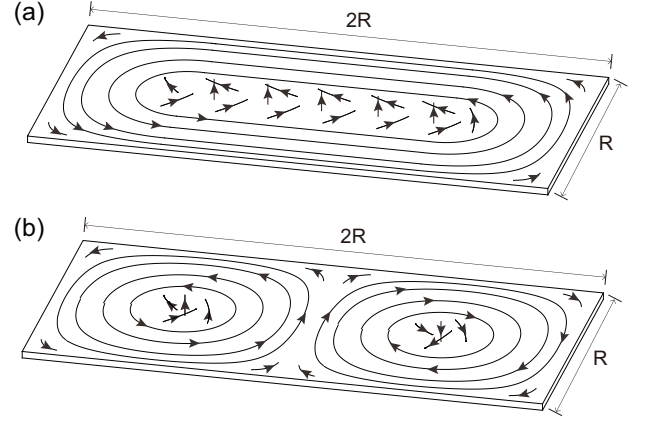


FIG. 5. In a large enough quasi-2D trap with an aspect ratio $q = 2$, the single meron in (a) costs more kinetic energy than the two antiparallel merons in (b).

shown in Fig. 5(a) costs a kinetic energy $\propto z_h R/R_{2D}$ near the center. Instead, the two-meron texture in Fig. 5(b) only costs a kinetic energy $\propto z_h \log(R/R_{2D})$, and thus will be favored at large R . The central spins of the two merons are aligned antiparallel to each other to further lower the DDI energy. Similarly, one may expect a q -meron spin texture to arise for a trap with aspect ratio q , which agrees well with the numerical results obtained in Ref. [9].

V. CONCLUSION

In conclusion, we have shown that the duality to the Dirac string gas picture is an efficient semi-analytical way of determining the spontaneous spin texture in a dipolar spinor condensate. The total dipolar energy can be conveniently estimated in the perspective of Dirac strings. Closed Dirac strings with curvatures as small as possible are generically preferred in the ground state. We expect this method to be further employed in future work to study the spin textures in external fields and the dynamics of spin textures. In addition, it will also be useful and intriguing to examine the possibility of constructing a quantum version of this duality as a generalization of the mean-field level duality presented here.

VI. ACKNOWLEDGEMENTS

The author thanks Prof. S. C. Zhang for carefully reading the manuscript, and the referees for their valuable suggestions.

Appendix A: Mean field description of ferromagnetic spinor condensates

Spin F bosons with DDI are most generally described by a Hamiltonian $\mathcal{H} = \mathcal{H}_0 + \mathcal{H}_D$, where \mathcal{H}_0 represents the kinetic energy and the local interaction [16], and \mathcal{H}_D is the long range DDI. In terms of the boson annihilation (creation) operators $\psi = (\psi_F, \dots, \psi_{-F})^T$, \mathcal{H}_0 is given by

$$\mathcal{H}_0 = \int d^3\mathbf{r} \left[\psi^\dagger \left(-\frac{\hbar^2 \nabla^2}{2M} - \mu \right) \psi + \sum_{J=0}^F g_{2J}^I \hat{P}_{2J} \right], \quad (\text{A1})$$

where $\hat{P}_{2J} = \sum_m (\psi^\dagger \otimes \psi^\dagger) |2J, m\rangle \langle 2J, m| (\psi \otimes \psi)$ is the local two-particle interaction projected into the total spin $2J$ channel, and g_{2J}^I is the corresponding interaction strength, and $g_{2J}^I = 2\pi\hbar^2 a_{2J}/M$ in terms of the s-wave scattering length a_{2J} . The whole Hamiltonian is $U(1) \times SU(2)$ symmetric. In the mean-field approximation, $\langle \psi_m(\mathbf{r}) \rangle = \Psi_m(\mathbf{r})$, where $\Psi_m(\mathbf{r}) = \sqrt{n(\mathbf{r})} \varphi_m(\mathbf{r})$ is the spinor order parameter. The mean field energy of \mathcal{H}_0 can then be written in the form

$$\mathcal{H}_0 = \int d^3\mathbf{r} \left[\frac{\hbar^2}{2M} |\nabla \sqrt{n(\mathbf{r})} \varphi(\mathbf{r})|^2 + V(n(\mathbf{r}), \varphi(\mathbf{r})) \right], \quad (\text{A2})$$

where $V(n, \varphi)$ is invariant under $U(1) \times SU(2)$ transformations of φ . For a ferromagnetic spinor condensate, both the $U(1)$ and $SU(2)$ symmetries are spontaneously broken, and there are two Goldstone modes corresponding to the $U(1)$ phase fluctuation and the spin direction fluctuation respectively [16]. At low energies, by integrating out the quantum fluctuation in density $n(\mathbf{r})$ in the path integral formalism, we can reduce the mean-field energy (A2) to

$$\begin{aligned} H_0 &= \int d^3\mathbf{r} \left[\frac{\hbar^2 (\partial_t \phi_{SF})^2}{4(\partial^2 V / \partial n^2)} + \frac{\hbar^2 n_0}{2M} |\nabla \varphi|^2 \right] \\ &= \int d^3\mathbf{r} \left[\frac{\hbar^2 (\partial_t \phi_{SF})^2}{4(\partial^2 V / \partial n^2)} + \frac{\hbar^2 n_0}{2M} (\nabla \phi_{SF})^2 + \frac{\alpha}{M} (\nabla \mathcal{F})^2 \right], \end{aligned} \quad (\text{A3})$$

where $\phi_{SF}(\mathbf{r})$ is the $U(1)$ phase, $\mathcal{F}(\mathbf{r}) = \varphi^\dagger \mathbf{F} \varphi / F_0$ is the normalized local spin, and the coefficient can be determined to be $\alpha = n_0 \hbar^2 [F(F+1) - F_0^2]/4$. We note that the local interactions g_{2J}^I only contribute to the parameter $\partial^2 V / \partial n^2$ in the first time dependent term, and do not enter the expression of the coefficient α .

Similarly, the mean field DDI energy H_D in Eq. (1) can be deduced by substituting the operator ψ_m with the mean field value $\Psi_m = \sqrt{n_0} \varphi_m$.

Since the DDI only depends on the spin field $\mathcal{F}(\mathbf{r})$, the ground state always tends to have a constant $U(1)$ phase ϕ_{SF} provided the spin field $\mathcal{F}(\mathbf{r})$ is smooth enough. Therefore, the effective low energy Hamiltonian of the system reduces to Eq. (1).

Appendix B: The kinetic energy H_0 rewritten in the Dirac string picture

To interpret the kinetic energy H_0 in the Dirac string picture, we first note that it can be rewritten as

$$\begin{aligned} H_0 &= -\frac{\alpha}{M} \int d^3\mathbf{r} \mathcal{F}(\mathbf{r}) \cdot \nabla^2 \mathcal{F}(\mathbf{r}) \\ &= -\frac{\alpha}{M} \int d^3\mathbf{r}_1 d^3\mathbf{r}_2 \delta(\mathbf{r}_1 - \mathbf{r}_2) \mathcal{F}(\mathbf{r}_2) \cdot \nabla_1^2 \mathcal{F}(\mathbf{r}_1), \end{aligned} \quad (\text{B1})$$

where ∇_1^2 is the Laplace operator with respect to \mathbf{r}_1 . In the Dirac string picture, we can write the volume element $d^3\mathbf{r}_i$ as $dl_i d\sigma_i$, and we have $\mathcal{F}(\mathbf{r}_i) = d\mathbf{r}_i / dl_i$, for $i = 1, 2$. The kinetic energy then becomes

$$H_0 = -\frac{\alpha}{M} \int d\sigma_1 d\sigma_2 dl_1 dl_2 \delta(\mathbf{r}_1 - \mathbf{r}_2) \frac{d\mathbf{r}_2}{dl_2} \cdot \nabla_1^2 \frac{d\mathbf{r}_1}{dl_1}. \quad (\text{B2})$$

By partial integrating the expression two times, we find

$$\begin{aligned} H_0 &= -\frac{\alpha}{M} \int d\sigma_1 d\sigma_2 dl_1 dl_2 \frac{d\mathbf{r}_2}{dl_2} \cdot \frac{d\mathbf{r}_1}{dl_1} \nabla_1^2 \delta(\mathbf{r}_1 - \mathbf{r}_2) \\ &= \frac{\alpha}{M} \int d\sigma_1 d\sigma_2 dl_1 dl_2 \left[1 - \frac{d\mathbf{r}_2}{dl_2} \cdot \frac{d\mathbf{r}_1}{dl_1} \right] \\ &\quad \times [\nabla_\perp^2 \delta(\mathbf{r}_1 - \mathbf{r}_2) + \partial_{l_1}^2 \delta(\mathbf{r}_1 - \mathbf{r}_2)] \\ &= \frac{\alpha}{M} \int d\sigma_1 d\sigma_2 dl_1 dl_2 \left[1 - \frac{d\mathbf{r}_2}{dl_2} \cdot \frac{d\mathbf{r}_1}{dl_1} \right] \\ &\quad \times \nabla_\perp^2 \delta(\mathbf{r}_1 - \mathbf{r}_2) - \frac{\alpha}{M} \int d\sigma_1 dl_1 \frac{d\mathbf{r}_1}{dl_1} \cdot \frac{d^3\mathbf{r}_1}{dl_1^3} \\ &= \frac{\alpha}{M} \int d\sigma_1 d\sigma_2 dl_1 dl_2 \left[1 - \frac{d\mathbf{r}_2}{dl_2} \cdot \frac{d\mathbf{r}_1}{dl_1} \right] \\ &\quad \times \nabla_\perp^2 \delta(\mathbf{r}_1 - \mathbf{r}_2) + \frac{\alpha}{M} \int d\sigma dl \left(\frac{d^2\mathbf{r}}{dl^2} \right)^2, \end{aligned} \quad (\text{B3})$$

where $\nabla_\perp^2 = \nabla^2 - \partial_{l_1}^2$. As is seen, the first term is a non-negative contact interaction between two Dirac strings, while the second term is an additional contribution to the self-energy of a Dirac string.

Appendix C: Numerical calculations of spin texture in spherical traps

In Eq. (9) we have derived an estimation of the total energy of the spin texture in a spherical trap from the Dirac string perspective, and show that the meron texture has a core size $R_0 = (8\alpha/3\lambda M)^{1/3} R^{1/3}$. Here we present a more accurate numerical calculation of the configuration of the meron texture. Based on the reasoning given in the main text, the following spin texture ansatz is appropriate, written in spherical coordinates (ρ, ϕ, z) as:

$$\mathcal{F}(\mathbf{r}) = \mathbf{e}_\phi \cos \zeta(\rho) + \mathbf{e}_z \sin \zeta(\rho), \quad (\text{C1})$$

bounded in the square well trap $\rho^2 + z^2 \leq R^2$. As is shown in Fig. 2(b), the monopole charges of this ansatz

are distributed on the surface of the trap, with an amount $\pm n_A \rho d\rho d\phi \sin \zeta(\rho)$ in the projected area $\rho d\rho d\phi$, where we have defined $n_A = g_F \mu_B n_0 F_0$. The total energy of the spin texture is then the summation of the string self energy, the kinetic energy and the monopole energy:

$$\begin{aligned} E_{3D} &= -\frac{\lambda}{6}V + \int d^3\mathbf{r} \frac{\alpha}{M} (\nabla \mathcal{F})^2 + E_Q \\ &= -\frac{\lambda}{6}V + \int_0^R d\rho \rho \sqrt{R^2 - \rho^2} \frac{4\pi\alpha}{M} \left[\left(\frac{d\zeta}{d\rho} \right)^2 + \frac{\cos^2 \zeta}{\rho^2} \right] \\ &\quad + \int_0^R d\rho d\rho' \int_0^{2\pi} d\phi \frac{\lambda \rho \rho' \sin \zeta \sin \zeta'}{2\sqrt{2}} \left(\frac{1}{D_+} - \frac{1}{D_-} \right), \end{aligned} \quad (\text{C2})$$

where

$$D_{\pm} = \sqrt{R^2 - \rho \rho' \cos \phi \pm \sqrt{(R^2 - \rho^2)(R^2 - \rho'^2)}}, \quad (\text{C3})$$

and we have used the abbreviations $\zeta = \zeta(\rho)$, $\zeta' = \zeta(\rho')$. $\sqrt{2}D_{\pm}$ has the physical meaning of the distance between two monopole charges (+ for charges on the same hemisphere, - for charges on the opposite hemisphere). The integration $\int d\phi/D_{\pm}$ can be expressed in terms of the elliptic K function to further simplify the energy functional.

This energy functional of $\zeta(\rho)$ can be minimized via the steepest descent method. In practice, we start with an arbitrary function of $\zeta(\rho)$, and add to the function an increment

$$\delta\zeta(\rho) = -\epsilon \nabla_{\zeta(\rho)} E_{3D},$$

repeatedly until the process converges, where ϵ is a small number. Provided ϵ is small enough, the numerical calculation converges well. The resulting functions $\zeta(\rho)$ for various values of R_0 are shown in Fig. 3.

-
- [1] J. Stuhler, A. Griesmaier, T. Koch, M. Fattori, T. Pfau, S. Giovanazzi, P. Pedri, and L. Santos, Phys. Rev. Lett. **95**, 150406 (2005).
 - [2] M. Lu, N. Q. Burdick, S. H. Youn, and B. L. Lev, Phys. Rev. Lett. **107**, 190401 (2011).
 - [3] K. Aikawa, A. Frisch, M. Mark, S. Baier, A. Rietzler, R. Grimm, and F. Ferlaino, Phys. Rev. Lett. **108**, 210401 (2012).
 - [4] M. Vengalattore, S. R. Leslie, J. Guzman, and D. M. Stamper-Kurn, Phys. Rev. Lett. **100**, 170403 (2008).
 - [5] M. Vengalattore, J. Guzman, S. R. Leslie, F. Serwane, and D. M. Stamper-Kurn, Phys. Rev. A **81**, 053612 (2010).
 - [6] J. Kronjäger, C. Becker, P. Soltan-Panahi, K. Bongs, and K. Sengstock, Phys. Rev. Lett. **105**, 090402 (2010).
 - [7] Y. Eto, H. Saito, and T. Hirano, Phys. Rev. Lett. **112**, 185301 (2014).
 - [8] S. Yi and H. Pu, Phys. Rev. Lett. **97**, 020401 (2006).
 - [9] J. Zhang and T.-L. Ho, J. Low Temp. Phys. **161**, 325 (2010).
 - [10] M. Takahashi, S. Ghosh, T. Mizushima, and K. Machida, Phys. Rev. Lett. **98**, 260403 (2007).
 - [11] Y. Kawaguchi, H. Saito, K. Kudo, and M. Ueda, Phys. Rev. A **82**, 043627 (2010).
 - [12] J. A. M. Huhtamäki, M. Takahashi, T. P. Simula, T. Mizushima, and K. Machida, Phys. Rev. A **81**, 063623 (2010).
 - [13] T.-L. Ho, Phys. Rev. Lett. **81**, 742 (1998).
 - [14] T. Ohmi and K. Machida, J. Phys. Soc. Jpn. **67**, 1822 (1998).
 - [15] Y. Kawaguchi and M. Ueda, Phys. Rev. A **84**, 053616 (2011).
 - [16] B. Lian, T.-L. Ho, and H. Zhai, Phys. Rev. A **85**, 051606 (2012).
 - [17] M. B. Green, J. H. Schwarz, and E. Witten, *Superstring Theory*, Vol. 1 (Cambridge U. P., Cambridge, 1987) pp. 22,47–49.
 - [18] Here the attraction between monopoles on the north pole and those on the south pole is neglected, which is around $-\lambda R_0^4/R$ and therefore smaller by a factor R_0/R .
 - [19] More precisely, the monopole energy (the third term of $E_{2D}^{(II)}$) is $(\pi\lambda/2)R_{2D}^2(R_{2D} + z_h - \sqrt{R_{2D}^2 + z_h^2})$.